Available online at www.sciencedirect.com
ScienceDirect
Journal of Power Sources 166 (2007) 149–154
JOURNAL OF POWER SOURCES
www.elsevier.com/locate/jpowsour

Short communication

Effect of clamping pressure on the performance of a PEM fuel cell

W.R. Chang [a], J.J. Hwang [b,*], F.B. Weng [c], S.H. Chan [c]

[a] *Department of Landscape Architecture, Chung-Hua University, Hsinchu 300, Taiwan*
[b] *Department of Environment and Energy, National University of Tainan, Tainan 700, Taiwan*
[c] *Fuel Cell Center and Department of Mechanical Engineering, Yuan Ze University, Nei Li, Taoyuan 320, Taiwan*

Received 2 December 2006; received in revised form 23 December 2006; accepted 2 January 2007
Available online 16 January 2007

Abstract

Examined were the effects of the clamping pressure on the performance of a proton exchange membrane (PEM) fuel cell. The electro-physical properties of the gas diffusion layer (GDL) such as porosity, gas permeability, electrical resistance and thickness were measured using a special-designed test rig under various clamping pressure levels. Correlations for the gas permeability of the GDL were developed in terms of the clamping pressure. In addition, the contact resistance between the GDL and the bipolar (graphite) plate was measured under various clamping pressures. Results showed that at the low clamping pressure levels (e.g. <5 bar) increasing the clamping pressure reduces the interfacial resistance between the bipolar plate and the GDL that enhances the electrochemical performance of a PEM fuel cell. In contrast, at the high clamping pressure levels (e.g. >10 bar), increasing the clamping pressure not only reduces the above Ohmic resistance but also narrows down the diffusion path for mass transfer from gas channels to the catalyst layers. Comprising the above two effects did not promote the power density too much but reduce the mass-transfer limitation for high current density.

Keywords: Proton exchange membrane fuel cell; Electro-physical properties; Clamping pressure

1. Introduction

In a common manufacture process, an electrolyte membrane is sandwiched between two gas diffusion layers (GDLs) using hot pressing to laminate a membrane-electrode assembly (MEA). The catalyst layer is in good contact with the electrolyte membrane as well as the GDL in a well-fabricated MEA [1]. That is the interfacial resistance (i.e., contact resistance) between the GDL and the electrolyte membrane may be neglected. In contrast, the MEA and the bipolar plates are separated in nature. The only way to assemble these two components together is the external mechanical force, i.e., the clamping pressure exerted on the endplates. Thus, the interfacial resistance between the GDL and the bipolar plate may be significant. It strongly depends on the external clamping force exerted on the endplates. In addition, since the GDL is a porous medium (usually, is made of carbon fiber papers or carbon clothes), it is highly sensitive to the clamping pressure. Not only is the thickness but also the porosity/permeability of the GDL changed due to the external clamping pressures. The above two factors strongly affect the electrochemical performance of a PEM fuel cell through influencing the Ohmic and *mass-transport polarizations* inside the fuel cell [1].

Quite a few experimental and numerical researches have been performed to figure out the effect of compression on the electrochemical performance of PEM fuel cells [2–6]. Based on the previous results, some design concepts have been deduced to build a reliable fuel cell system by considering the interfacial contact resistance as well as the reactant-fluid transport under various compression conditions. However, the effect of the clamping pressure on the electro-physical properties such as porosity and permeability of the GDL has not been discussed yet. In addition, the dependence of the contact resistance between the GDL and the bipolar plate on the clamping pressure is quite uncertain according to the results in the open literature.

The object of this paper is to experimentally study the effect of clamping force on the performance of a PEM fuel cell. Two tasks are carried out in the present study. The first one is to experimentally examine the effect of the clamping pressure on the electro-physical properties of a carbon paper GDL such as

* Corresponding author. Tel.: +886 62600321; fax: +886 62602596.
E-mail address: azaijj@mail.nutn.edu.tw (J.J. Hwang).

0378-7753/$ – see front matter © 2007 Elsevier B.V. All rights reserved.
doi:10.1016/j.jpowsour.2007.01.015

Nomenclature

A	area of the GDL sample (m^2)
F	Faraday's constant
I	current density ($A\,m^{-2}$)
K_a	Kozeny constant
M	molecular weight ($kg\,mol^{-1}$)
P	pressure (Pa)
Q	mass flow rate ($kg\,s^{-1}$)
r_1	i.d. of the GDL sample (m)
r_2	o.d. of the GDL sample (m)
R	universal gas constant ($W\,mol^{-1}\,K^{-1}$)
$R_{BP/Cu}$	contact electrical resistance between the copper plate and the bipolar plate ($\Omega\,m^2$)
$R_{BP/GDL}$	contact electrical resistance between the GDL and the bipolar plate ($\Omega\,m^2$)
R_{total}	total electrical resistance ($\Omega\,m^2$)
R_Ω	through-plane electrical resistance of the GDL sample ($\Omega\,m^2$)
T	temperature (K)
u_r	radial velocity ($m\,s^{-1}$)

Greek symbols

ε	porosity
κ	gas permeability (m^2)
μ	dynamic viscosity ($m\,s^{-2}$)
ρ	density ($kg\,m^3$)

porosity and gas permeability. The electrical contact resistance between the GDL and its neighboring bipolar plate are measured as well. These drastic changes of GDL characteristics could have a remarkable effect on the fuel cell performance. Thus, it is very important to find how the variation of the above electro-physical properties in the GDL goes through under different clamping pressures, targeting to elucidate the intrinsic characteristics of carbon paper which is widely used in modeling of a PEM fuel cell. The second task of this paper is to examine the effects of clamping pressure on the electrochemical performance of a PEM fuel cell for different operating conditions. During the final assembly phase of a fuel cell stack, clamping pressure exerted on the endplates of a cell-assembly makes a close contact between the components, building a sole power-generation unit. It is of great importance to adjust the applied clamping pressure to keep the close contact between the core elements to a favorable extent.

2. Experimental setup

The present experimental study focused on the effect of clamping forces on the electrochemical performance of a PEM fuel cell. Before the electrochemical test of a PEM fuel cell stack, electro-physical properties of the GDL under various clamping pressure were evaluated. As depicted in Fig. 1, an integrated multi-purpose test stand was devised to measure electrical resistance, thickness, porosity, and gas permeability of the GDL. A load cell can weigh the external load up to maximum 200 kg.

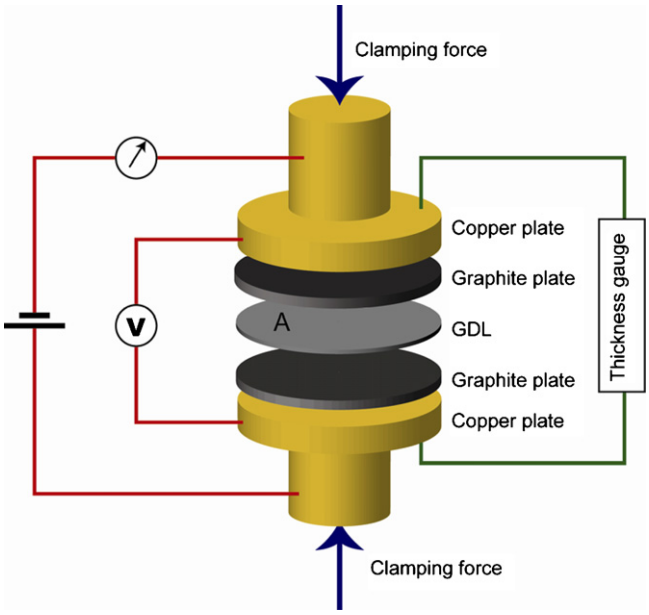

Fig. 1. Schematic drawing of the clamping pressure test.

A milliohm meter (Agilent Technologies, with a minimum of $1 \times 10^{-5}\,\Omega$) was employed to measure the electrical resistance across the assembly between two copper plates. The thickness variation of carbon papers was monitored using a thickness gauge which has a minimal gauging limit of 1.0 μm.

2.1. Contact resistance measurement

A GDL specimen with an initial thickness of 120 μm was placed between two graphite plates, each of which was in contact with a copper plate on the opposite side. While a constant current was passed through the two copper plates, the electrical potential difference between the copper plates was measured. The measurement was repeated at various clamping pressures applied through the apparatus, in order to examine its effects on the contact resistance. The total electrical resistance across the assembly in Fig. 1 was calculated based on the Ohm's law.

$$R_{total} = \frac{VA}{I} \tag{1}$$

where A is the surface area of the GDL specimen. An additional measurement was conducted to determine a reference electrical resistance without the GDL sample, $R_{BP/Cu}$. That is a graphite plate of double thickness was inserted between the copper plates. It well represents a combination of the contact resistances between two copper plates and the graphite plate and the electrical resistance of the graphite plate itself. Thus, the contact electrical resistance between the graphite plate and the GDL can be expressed as

$$R_{BP/GDL} = \tfrac{1}{2}(R_{total} - R_\Omega - R_{BP/Cu}) \tag{2}$$

where R_Ω is the through-plane electrical resistance of the GDL sample.

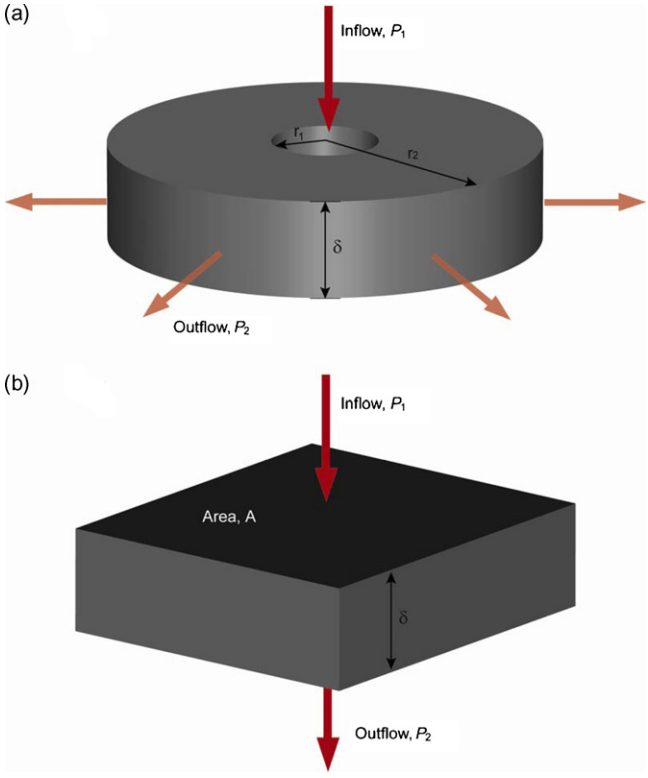

Fig. 2. Schematic drawing of the gas permeability measurements: (a) in-plane gas permeability and (b) through-plane gas permeability.

2.2. Porosity and gas permeability of GDL

Fluid flow in the GDL encounters additional flow resistance which causes momentum losses by the intrinsic characteristics of the porous media. This momentum loss is closely related to the microstructure, material characteristics, porosity, and the gas permeability of the GDLs. However, it is hard to quantify the momentum losses of a fluid. Therefore, we need to identify the electro-physical properties describing the diminution of a vector field through a porous media.

A schematic drawing of the measurements of gas permeabilities of a GDL is given in Fig. 2. The donut sample and the rectangle sample are used to determine the in-plane and through-plane gas permeabilities, respectively. They were determined by using the pressure-drop across the porous sample together with the mean flow rate in the porous medium under an isothermal condition.

As for the in-plane gas permeability measurement, the geometry of the GDL sample is a concentric circle with o.d. $r_2 = 25.4$ mm and i.d. $r_1 = 5.08$ mm, respectively. During the compression process, the external compressive force was determined using the load cell, while the thickness of the GDL specimen was monitored using a thickness gauge. Pressurized air enters the GDL from the central hole and then diffuses peripherally to atmosphere. A pressure conditioner with a resolution of 0.001 bar and a mass flow controller (Brooks) were equipped to measure the pressure-drop across and the flow rate across the sample, respectively. Note that before entering the test sample, the pressurized air passed through a moisture removing filter packed with dendrites to eliminate the effect of humidity on the gas permeability. The gas velocity in the GDL was calculated by measuring pressure before infusing into the concentric porous media by Darcy's law [7,8],

$$u_r = \frac{\kappa}{\mu}\nabla P \tag{3}$$

where u_r represents the radial velocity vector, κ the gas permeability, μ the molecular viscosity, and P represents the pressure, respectively.

Considering the pressure gradient along the radial direction only,

$$\frac{\partial P}{\partial r} = -\frac{\mu}{\kappa}u_r \tag{4}$$

The gas mass flow rate is

$$Q_r = \rho u_r 2\pi r\delta \tag{5}$$

where δ represents the thickness of the GDL. Thus, the radial velocity vector given as follows:

$$u_r = \frac{1}{2\pi r\delta}\frac{RT}{PM}Q \tag{6}$$

where R is the universal gas constant, T the temperature, and M is the molecular weight of the air, respectively. Combining Eqs. (4) and (6) gives

$$\frac{\partial P}{\partial r} = -\frac{\kappa}{\mu}\frac{1}{2\pi r\delta}\frac{RT}{PM}Q \tag{7}$$

The gas permeability of the GDL can be obtained by integrating the above equation, i.e.,

$$\kappa = \frac{RT}{M}\frac{\mu}{\pi\delta}\frac{Q}{P_1^2 - P_2^2}\ln\left(\frac{r_2}{r_1}\right) \tag{8}$$

where P_1 and P_2 correspond to the inlet pressure and the outlet pressure, respectively.

Accordingly, the through-plane gas permeability of the GDL was determined by using the following equation:

$$\kappa = 2\frac{RT}{M}\frac{\mu\delta}{A}\frac{Q}{P_1^2 - P_2^2} \tag{9}$$

where A is the area of the GDL sample.

The volume-based porosity (ε) of the GDL sample provided by the manufacturer is determined using the weight of the sample with the density of the carbon fibers. In this study, it is rechecked by determining the void-to-total volume ratio of the sample, in which the sample total volume is measured by its geometry and the pore volume is determined by filling water inside the sample. In addition, the porosity of a porous medium can be derived using Eq. (8) along with the Carman–Kozeny relation as follows:

$$\kappa = \frac{\varepsilon d_g}{K_a(1-\varepsilon)^2} \tag{10}$$

where d_g is the average diameter of carbon fibers and K_a is the Kozeny constant (can vary between 60 and 180, depending on the medium architecture). Note that the deviation between Eq. (9) the data from the manufacture is about 5.0%.

2.3. I–V curve measurements

After the measurements of the electro-physical characteristics of the GDL, focus will be turned to the effect of clamping forces on the electrochemical performance of a PEM fuel cell. All data reported here were obtained with self-made MEAs [1]. The catalyst layer was 30 μm in thickness and the active area was 25 cm^2, with 0.3 mg cm^{-2} Pt loading. The commercially available gas diffusion layers, toray, were used. The serpentine flow fields machined on the graphite plates consist of five equally spaced channels and bends for a total length of approximately 0.25 m between the entrance and the exit. The *I–V* curves are measured on a test station produced by Fuel Cell Technology. High purity hydrogen of 99.997% and compressed air were used as the anodic and cathodic feedings, respectively. The flow rates were adjusted automatically in an iterative manner to maintain a fixed stoichiometry according to the measured current. Two mass-flow controllers that were calibrated by using a bubble flow meter controlled the gas flow rates. The gas temperature and the degree of humidity were controlled by sparging the gases through water filled tanks held at a fixed temperature of 333 K for the both feedings. The temperature of the cell was also 333 K. The same operating temperatures were used for all experiments and temperature controllers were used to keep these as constants during experiments. Also, the pressures of the anode and cathode sides were both 1.1 bar. A break-in test using pure oxygen was carried out to ensure the cell performance was stable during the compression experiments. For a polarization curve the cell voltage was changed from 0.2 V to OCV and the resulting currents were recorded.

3. Results and discussion

3.1. Electro-physical properties of GDL

Fig. 3 shows the effect of clamping pressure on the porosity and thickness of the GDL. The GDL sample has 120 μm in thickness at its initial state. As shown in Fig. 3, the GDL thickness has a relatively stiff gradient in a low range of the

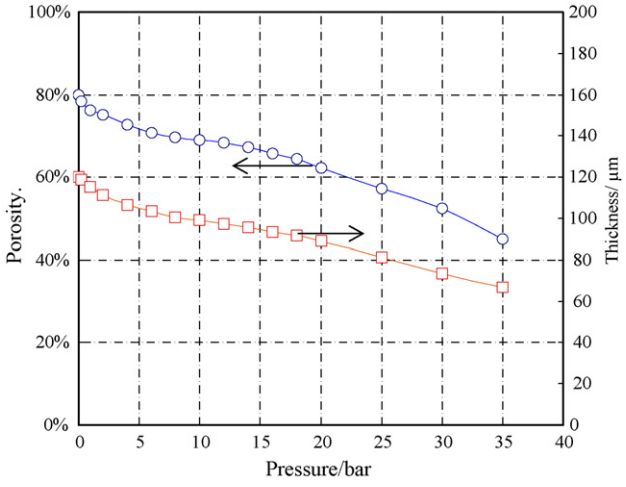

Fig. 3. Effect of pressure on the porosity and thickness of the gas diffusion layer.

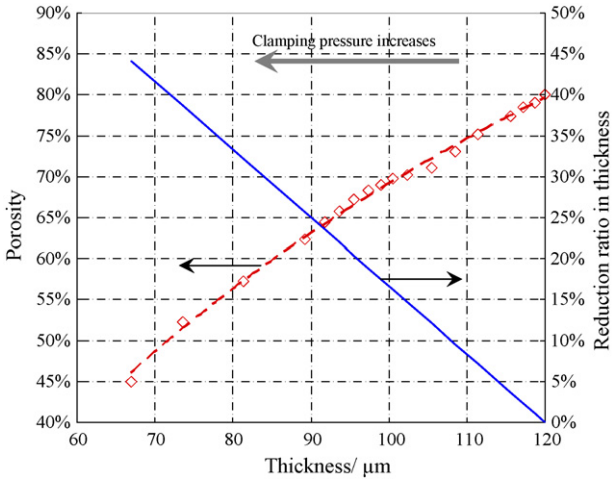

Fig. 4. Correlation of the porosity and thickness of the gas diffusion layer.

external clamping pressure (e.g. <5 bar), resulting in a relatively sharp decrease in porosity. In the remaining compression pressure ranges, the porosity of the GDL is inversely proportional to the external clamping pressure. It is further seen that at the clamping pressure of 35 bar, the thickness of the GDL is reduced by 45%. Considering practical applications, the carbon paper is reduced up to 20–30% in thickness for the clamping pressure ranged from 10 to 20 bar.

Fig. 4 further shows the porosity variation as a function of the thickness (δ) of the GDL. The diamond symbols are experimentally determined while the dashed curve is correlated from the experimental data. It can be represented by the following form:

$$\varepsilon = 1 - \exp\left[-\frac{(\delta - 24)}{60}\right] \tag{11}$$

At the initial state (without external pressure), i.e., $\delta = 120$ μm, the carbon paper normally has 0.80 in porosity. Physically, the lower limit in thickness of the GDL should be $\delta = 24$ μm, in which the porous matrix was compressed into a solid structure ($\varepsilon = 0$). From the above equation, the gradient of the porosity curve shows an exponential pattern as the clamping pressure increases, indicating that the carbon paper has a mild deformation in porosity with less thickness change and then severe shrinkage in the pore volume under the high clamping pressure range.

It should be noted that large porosities facilitate the mass diffusion through a porous medium, providing sufficient amounts of reactants to the catalyst layer. The external clamping load to a fuel cell stack results in the deflation of the vacant space of the porous carbon paper. In contrast, there is negligible variance in the volume of the solid carbon matrix and therefore porosity becomes smaller which resists mass transfer in the through-membrane direction, from the gas channels to the catalyst layer. In the practical range of fuel cells, the favorable compressed thickness of the carbon paper is close to 120 μm and the corresponding porosity equals to 0.75 with less than 5% change of porosity as shown in Fig. 4.

Fig. 5 shows the in-plane gas permeability of the GDL as a function of the external clamping pressure. As the clamp-

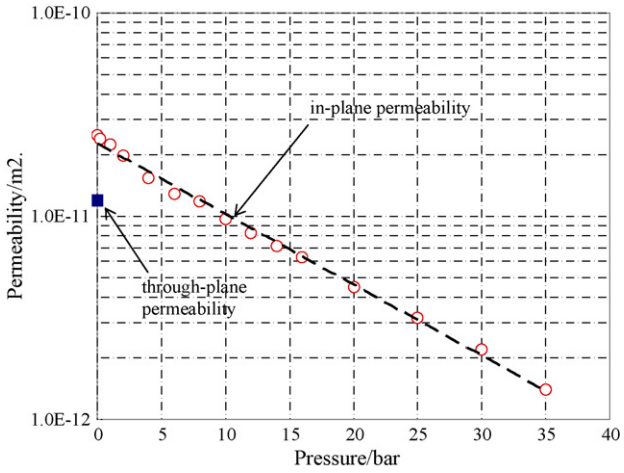

Fig. 5. Effect of pressure on the permeability of the gas diffusion layer.

ing pressure increases, the permeability shows an exponentially decreasing pattern. It can be represented by the following correlation (dashed line):

$$\kappa = \kappa_0 \exp\left(-0.0823\frac{F}{A}\right) \quad (12)$$

where κ_0 is the initial permeability of the carbon paper. As shown in Fig. 5, 5 bar of external pressure makes 50% change in gas permeability. Considering carbon-paper thickness variation in the fuel cell application, e.g. 30% compression of a carbon paper, the permeability significantly drops down to 1.0×1.0^{-12} from 2.5×10^{-11} at the initial state. When the carbon paper further goes through 50% compression in thickness, the permeability reduces down to 1/10 of the initial value. Since the examination of compression effect on the through-plane gas permeability is not available in the present facility, only the data under uncompressed conditions are obtained. The value plotted in Fig. 5 (solid square symbol) is the average of five replicates. It is found the through-plane gas permeability to be about a half of the in-plane value which is in agreement with the previous findings [6].

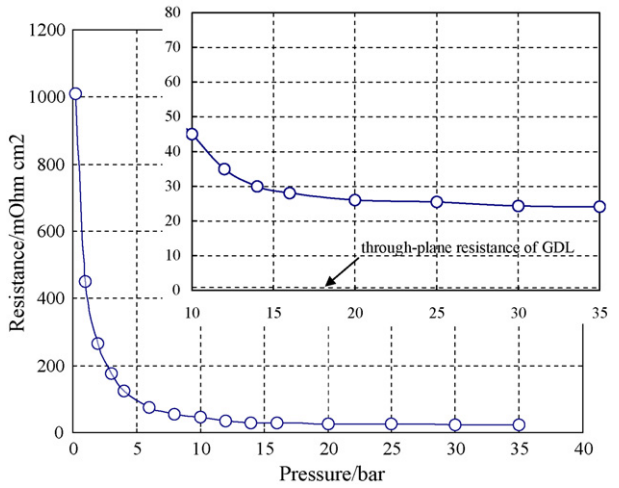

Fig. 6. Effect of pressure on the electrical resistance of the gas diffusion layer.

Fig. 6 shows the contact electrical resistance between GDL and bipolar plate ($R_{BP/GDL}$) as a function of the clamping pressure. The through-plane electrical resistance (dashed line) of the GDL sample is also provided for comparison. It is clearly seen that the through-plane resistance is quite small as compared to the contact electrical resistance. It is only about one-thirtieth of the asymptotic value of the contact resistance. The contact electrical resistance is sharply reduced down with a slight external clamping pressure from 1000 mΩ cm^2 at the initial state to 180 mΩ cm^2 at 2.5 bar and then shows an asymptotic curve converging on about 25 mΩ cm^2. Note that the leakage test reveals that no leakage occurs in the present module when the clamping pressure is higher than 2 bar. In the practical range of stacking pressure, e.g. 10 bar, the magnitude of electrical resistance becomes less than 50 mΩ cm^2 as shown in Fig. 6. In general, a fully hydrated Nafion 112 membrane has an electrical resistance of 70 mΩ cm^2 [1]. Therefore, it is evident that the interfacial contact resistance could be a considerable amount of electrical loss of fuel cells and thus it is necessary to clamp a fuel cell stack closely together with properly compression.

3.2. Electrochemical performance of a PEM fuel cell

Before measuring the single-cell polarization, a systematic leakage test was taken to determine the minimal compression for proper sealing. For each set of experiments, the fuel cell was assembled and the compression was set at a value a little above the pre-determined minimal compression to ensure good sealing. Then a leakage-check was performed to ensure a good seal. After the leakage-check, the fuel cell was run at pre-determined operating conditions. Then, the compression was increased a small amount and the test was repeated at the same operating conditions. This procedure continued until the pre-determined compression was reached. The operating conditions were as follows unless stated otherwise. For each compression condition, several tests were conducted to verify the performance was repeatable under the same operational conditions. Table 1 shows the configuration of the single cell and it operation condition.

Fig. 7 shows the dynamic behaviors of the current of the PEM fuel cell under three different clamping pressures. The cell voltage keeps at 0.6 V. It is seen that the current is dynamically stable for all three clamping pressures. The higher current accompanied by the higher clamping pressure may be attributed to the lower interfacial electrical resistance between the components

Table 1
Configuration of the single cell and its operation conditions

Description	Value
Configuration of electrode (active electrode area)	50 mm × 50 mm (25 cm^2)
Number of flow channels; configuration	Three, serpentine
Flow channel width	1 mm
Flow channel interval	1 mm
Flow channel depth	1 mm
Cell temperature	333 K
Stoichiometry, anode/cathode	1.5/3
Inlet relative humidity, anode/cathode	100%/100%
Operating pressure, anode/cathode	1.0 atm/1.0 atm

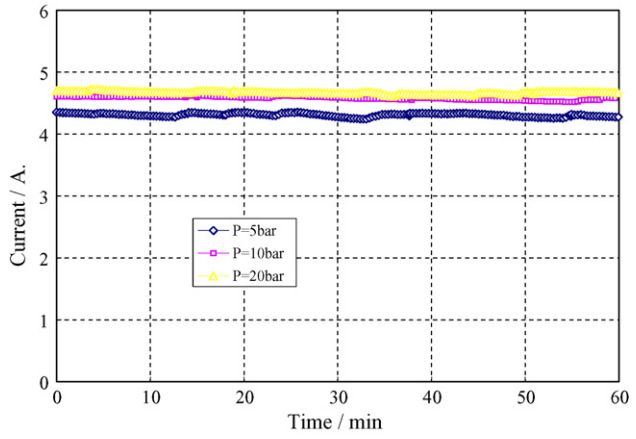

Fig. 7. Durability test for different clamping force applied to the PEM fuel cell.

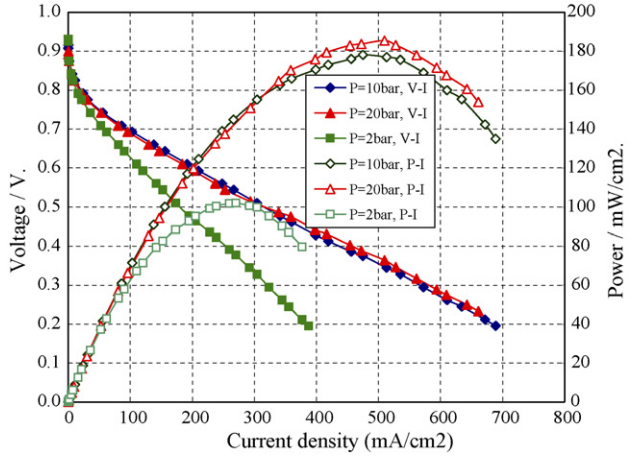

Fig. 8. Effect of pressure on the electrical resistance of the gas diffusion layer.

(Fig. 6). Fig. 8 further shows the performance curve for a single-cell experiment for three different clamping pressures. Again, the polarization curves can be considered to reflect the effect of the interfacial electrical resistance and mass transfer since the ionic conductivity has negligible variance under the operating condition of fully saturated fuel and oxidant feed stream. It is shown in Fig. 8 that the fuel cell performance appears worst with 2 bar clamping pressure. Compression between 10 and 20 bar shows a negligible difference in the performance curve between them. As shown in Fig. 6, the case of 10-bar compression has a slightly higher interfacial electrical resistance than the case of 20-bar compression, and thus shows a lower power density. However, the polarization curve for the case of 10-bar compression further shows the maximum limiting current density favorable from the mass transfer point of view [9]. In addition, since the thickness of GDL is reduced, the reactants are harder to penetrate into the region of GDL under the lands, which will lead to a severe non-uniform distribution of reactant over the whole electrode and thus increase the in-plane mass-transport polarization [10]. Actually, with further compression higher than 10-bar, it seems to be difficult to achieve more than 0.7 A cm^{-2} of current density due mainly to the mass-transfer limitation. Therefore, it can be concluded that the compression of carbon paper between 10 and 20 bar is the optimal clamping pressure of the present GDL sample.

4. Conclusions

The effects of changing the clamping pressure on the performance of a PEM fuel cell have been investigated experimentally. A special-designed test rig has successfully developed to simultaneously measure the thickness, gas permeability, and porosity of a GDL sample under various clamping pressure conditions. The contact electrical resistance between the graphite plate and the GDL sample is determined as well. Results show that the through-plane electrical resistance of the carbon paper itself is not significant. However, the contact resistance between the GDL and the bipolar plate is considerable that causes a serious potential loss across the fuel cells. An empirical correlation for gas permeability has been developed in terms of the clamping pressure. It is further shown that low clamping pressure results in a high interfacial resistance between the bipolar plate and the gas diffusion layer that reduces the electrochemical performance of a PEM fuel cell. In contrast, high clamping pressure reduces the contact resistance between the graphite plate and the gas diffusion layer, but meanwhile narrows down the diffusion path for mass transfer from gas channels to the catalyst layers. Comprising the above two effects did not promote the power density but reduce the mass-transfer limitation for high current density.

Acknowledgements

This work was partly sponsored by the National Science Council of Taiwan under contract no. NSC 94-2212-E-451-001.

References

[1] J.J. Hwang, H.S. Hwang, J. Power Sources 104 (2002) 24–32.
[2] W.K. Lee, C.H. Ho, J.W. Van Zee, M. Murthy, J. Power Sources 84 (1999) 45–51.
[3] S.P. Jiang, J.G. Love, L. Apateanu, Solid State Ionics 160 (2003) 15–26.
[4] R.F. Silva, D. Franchi, A. Leone, L. Pilloni, A. Masci, A. Pozio, Electrochim. Acta 51 (2006) 3592–3598.
[5] M.V. Williams, E. Begg, L. Bonville, H.R. Kunz, J.M. Fenton, J. Electrochem. Soc. 151 (2004) A1173–A1180.
[6] J. Ihonen, M. Mikkola, G. Lindbergh, J. Electrochem. Soc. 151 (2004) 1152–1161.
[7] J.J. Hwang, G.J. Hwang, R.H. Yeh, C.H. Chao, ASME, J. Heat Transfer 124 (2002) 120–129.
[8] J.J. Hwang, J. Electrochem. Soc. 153 (2006) A216–A224.
[9] J.J. Hwang, C.K. Chen, R.F. Savinell, C.C. Liu, J. Wainright, J. Appl. Electrochem. 34 (2004) 217–224.
[10] C. Xu, T.S. Zhao, Q. Ye, Electrochim. Acta 51 (2006) 5524–5531.